Supporting Information for:

Unidirectional imaging with partially coherent light

Guangdong Ma[1,2,3,4,†], Che-Yung Shen[1,2,3,†], Jingxi Li[1,2,3], Luzhe Huang[1,2,3], Çağatay Işıl[1,2,3], Fazil Onuralp Ardic[1], Xilin Yang [1,2,3], Yuhang Li[1,2,3], Yuntian Wang [1,2,3], Md Sadman Sakib Rahman[1,2,3], Aydogan Ozcan[*,1,2,3,5]

[1]Electrical and Computer Engineering Department, University of California, Los Angeles, CA, 90095, USA.

[2]Bioengineering Department, University of California, Los Angeles, 90095, USA.

[3]California NanoSystems Institute (CNSI), University of California, Los Angeles, CA, 90095, USA.

[4]School of Physics, Xi'an Jiaotong University, Xi'an, Shaanxi, 710049, China.

[5]Department of Surgery, University of California, Los Angeles, CA, 90095, USA.

[†]These authors contributed equally

*Correspondence: Aydogan Ozcan, ozcan@ucla.edu

Supplementary Figures

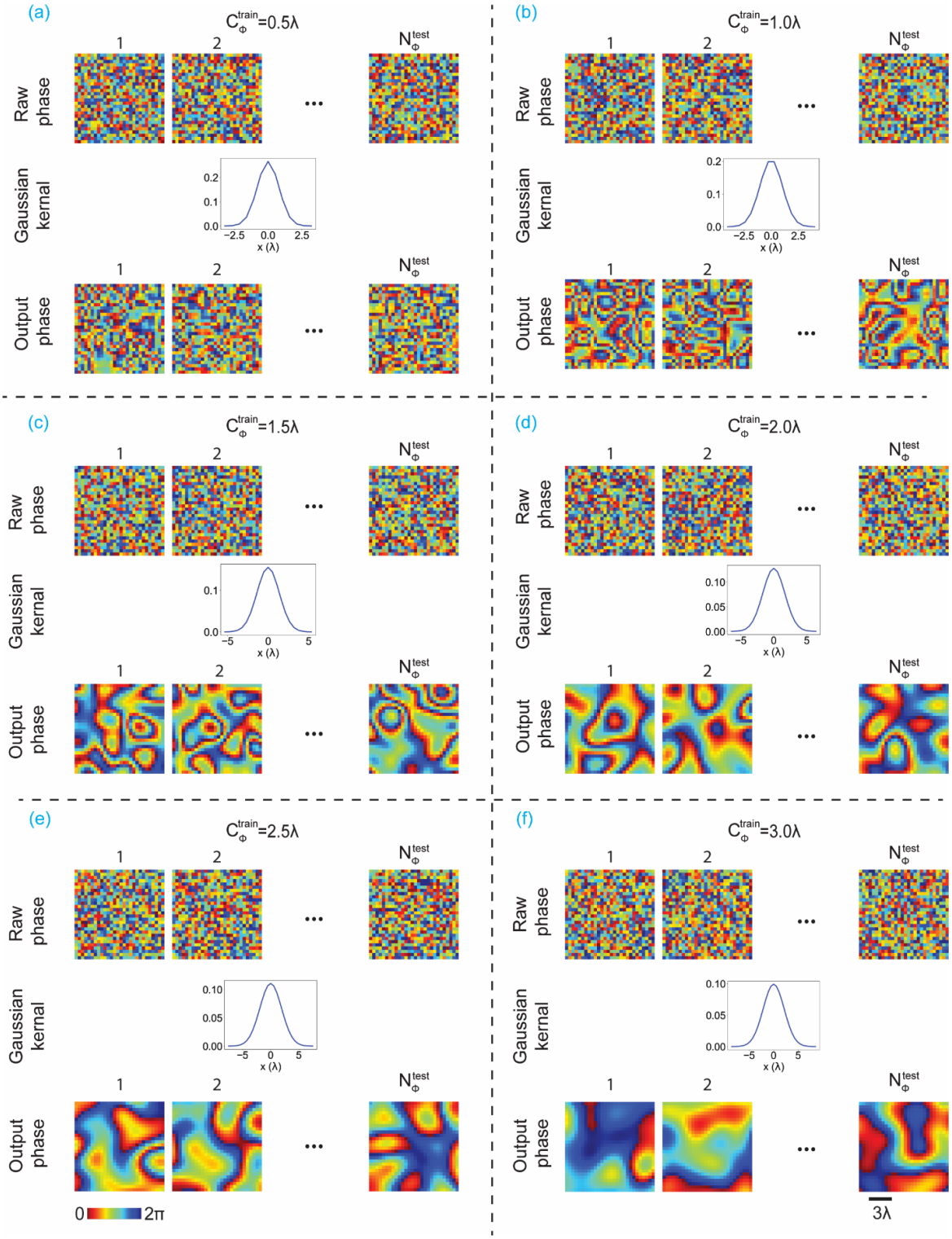

Figure S1 (a) – (f) Generation of N_ϕ^{test} random phase profiles with different phase correlation lengths - from $\sim 0.5\lambda$ to $\sim 3\lambda$. Also see the Methods section of the main text.

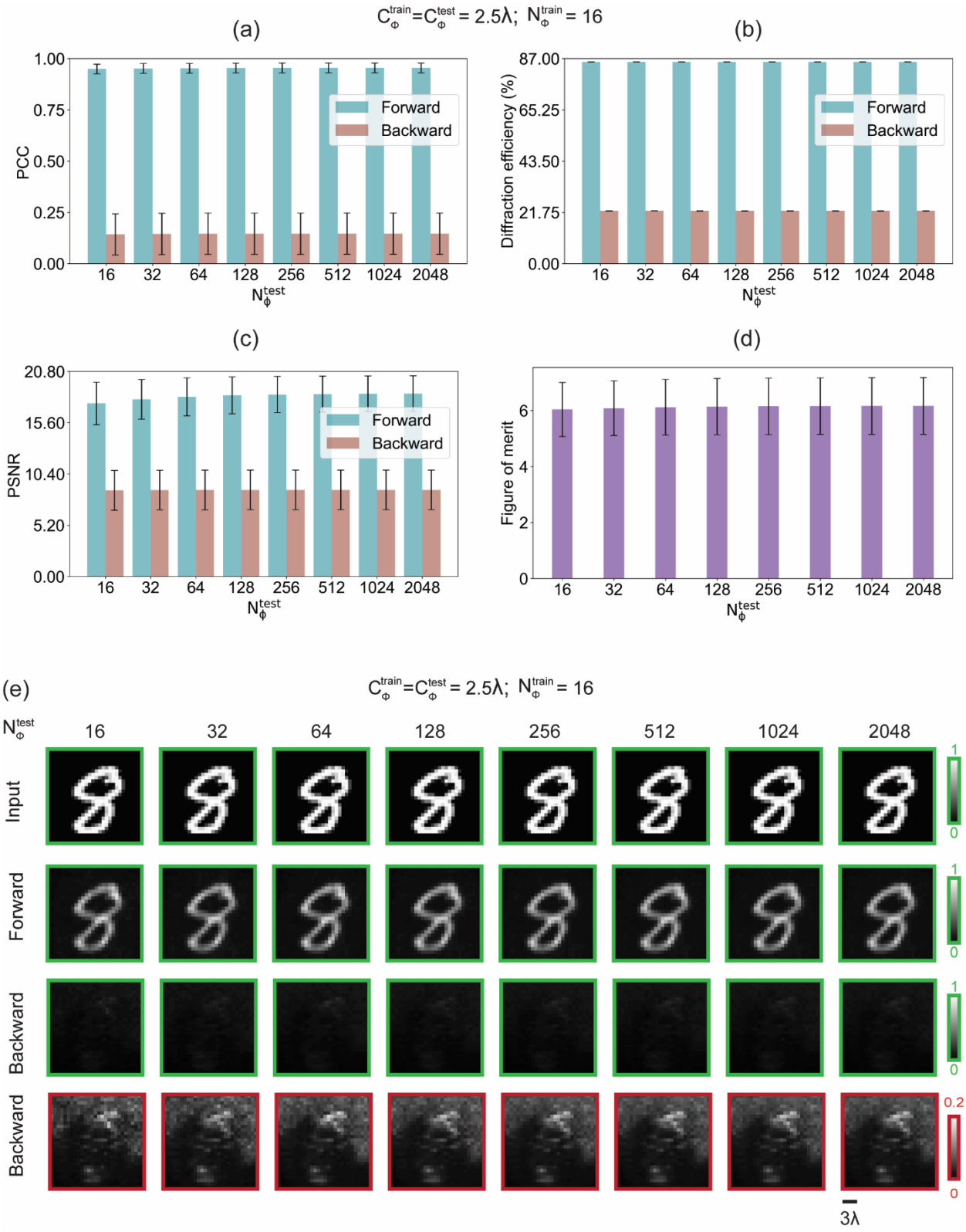

Figure S2. Impact of N_Φ^{test} on the performance of partially coherent unidirectional imagers. (a)-(d) Performance analysis of partially coherent unidirectional diffractive imagers with $C_\Phi^{train} = C_\Phi^{test} = 2.5\lambda$

and $N_{\Phi}^{train} = 16$, but for different N_{Φ}^{test} values ranging from 16 to 2048. The performance in each case was evaluated using 10,000 MNIST test images with PCC, diffraction efficiency, PSNR, and FOM metrics. (e) Examples of the blinding testing results with different N_{Φ}^{test} values ranging from 16 to 2048. The first three rows display the input amplitude objects, forward output images, and backward output images. For comparison, the last row shows the backward output images with different intensity ranges. Images with the same colored frame share the same intensity range.

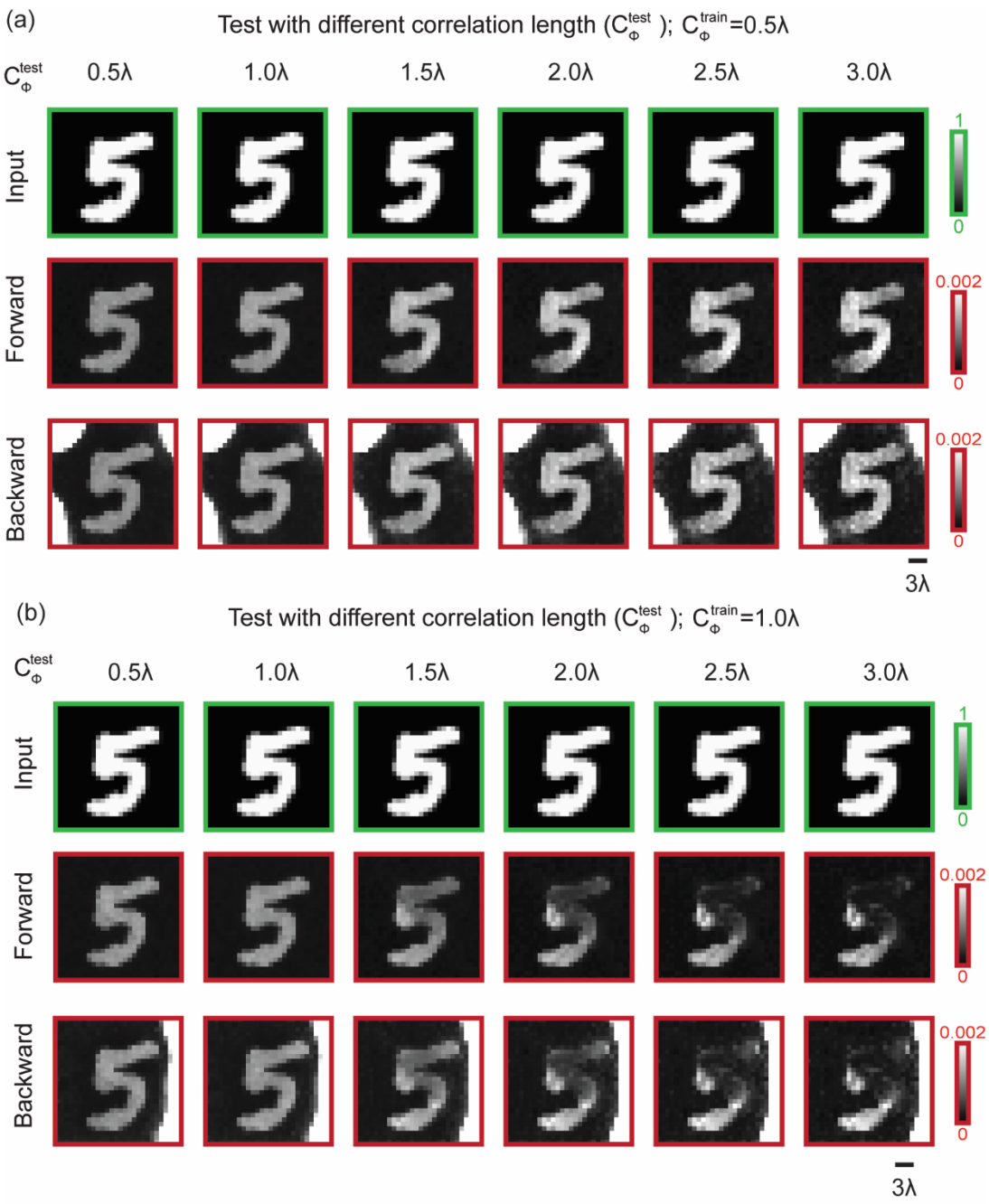

Figure S3. The performance of unidirectional diffractive imagers for various $\mathbf{C_\phi^{test}}$ values, varying from $\sim\mathbf{0.5}\boldsymbol{\lambda}$ to $\sim\mathbf{3}\boldsymbol{\lambda}$, despite being trained with a specific $\mathbf{C_\phi^{train}}$. (a) $C_\phi^{train} = 0.5\lambda$. (b) $C_\phi^{train} = 1.0\lambda$. Each part displays the input amplitude objects, forward output images, and backward output images. Images with the same colored frame share the same intensity range.

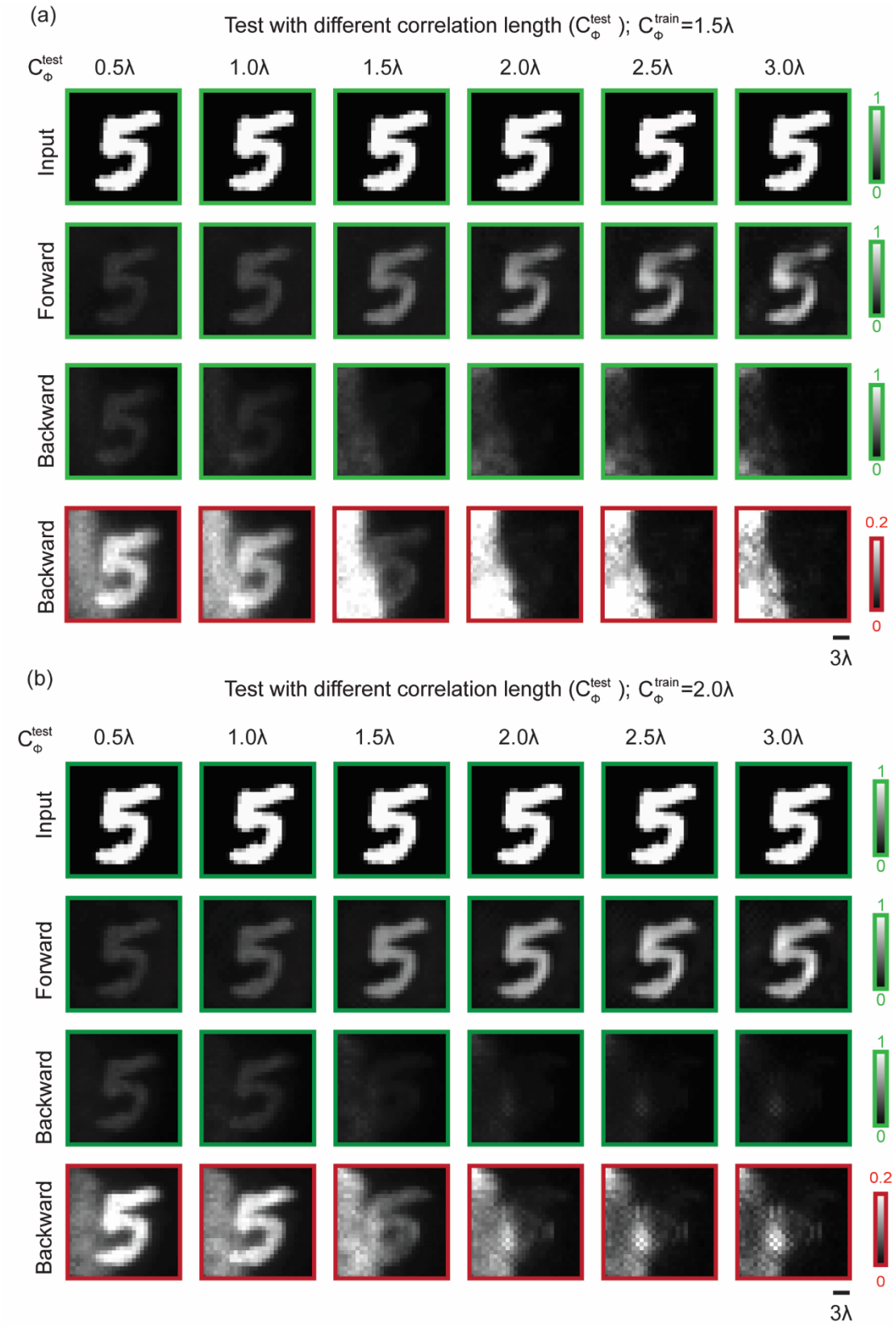

Figure S4. The performance of unidirectional diffractive imagers for various C_ϕ^{test} values, varying from

$\sim 0.5\lambda$ to $\sim 3\lambda$, despite being trained with a specific C_{ϕ}^{train}. (a) $C_{\phi}^{train} = 1.5\lambda$. (b) $C_{\phi}^{train} = 2.0\lambda$. The first three rows display the input amplitude objects, forward output images, and backward output images. For comparison, the last row shows the backward output images with different intensity ranges. Images with the same colored frame share the same intensity range.

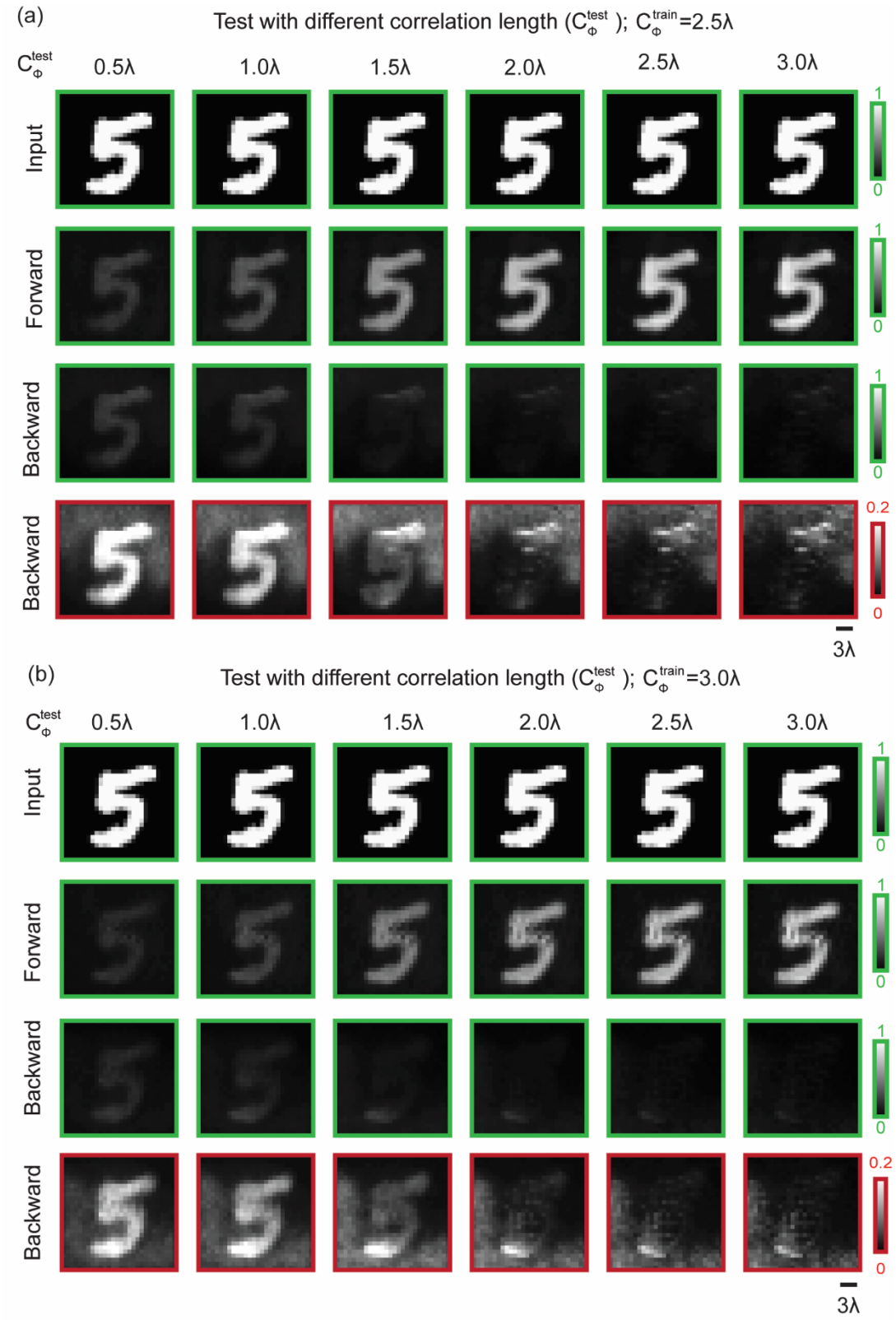

Figure S5. The performance of unidirectional diffractive imagers for various C_Φ^{test} values, varying from $\sim 0.5\lambda$ to $\sim 3\lambda$, despite being trained with a specific C_Φ^{train}. (a) $C_\Phi^{train} = 2.5\lambda$. (b) $C_\Phi^{train} = 3.0\lambda$. The first

three rows display the input amplitude objects, forward output images, and backward output images. For comparison, the last row shows the backward output images with different intensity ranges. Images with the same colored frame share the same intensity range.

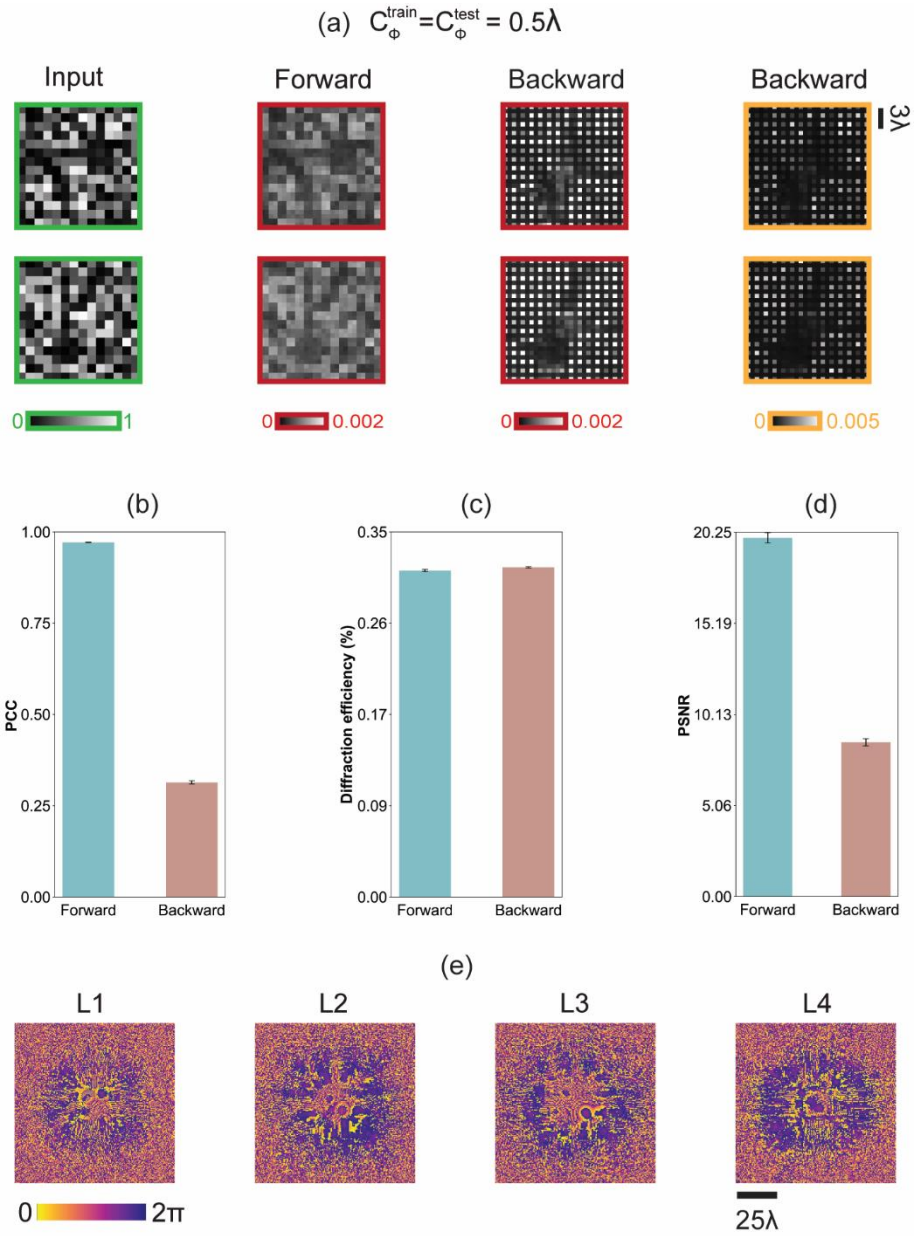

Figure S6 (a-d) Blind testing results of a unidirectional diffractive imager design with $C_\Phi^{train} = C_\Phi^{test} = 0.5\lambda$, when trained using a high resolution image dataset; see the Methods section of the main text. The first three columns in (a) display the input intensity objects, forward output images, and backward output images. For comparison, the last column in (a) shows the backward output images with different intensity

ranges. Images with the same colored frame share the same intensity range. (e) Optimized phase profiles of the diffractive layers. Each diffractive layer contains 200 × 200 diffractive features.

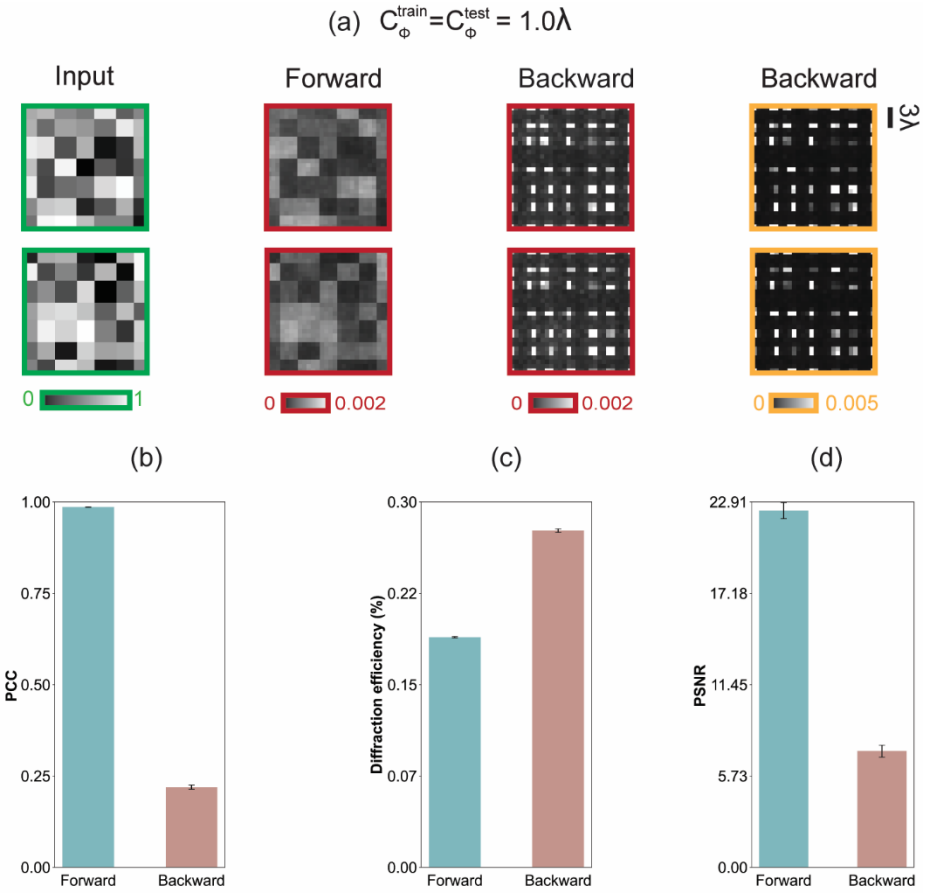

Figure S7 (a-d) Blind testing results of a unidirectional diffractive imager design with $C_\Phi^{train} = C_\Phi^{test} = 1.0\lambda$, when trained using a high-resolution image dataset; see the Methods section of the main text. The first three columns in (a) display the input intensity objects, forward output images, and backward output images. For comparison, the last column in (a) shows the backward output images with different intensity ranges. Images with the same colored frame share the same intensity range.

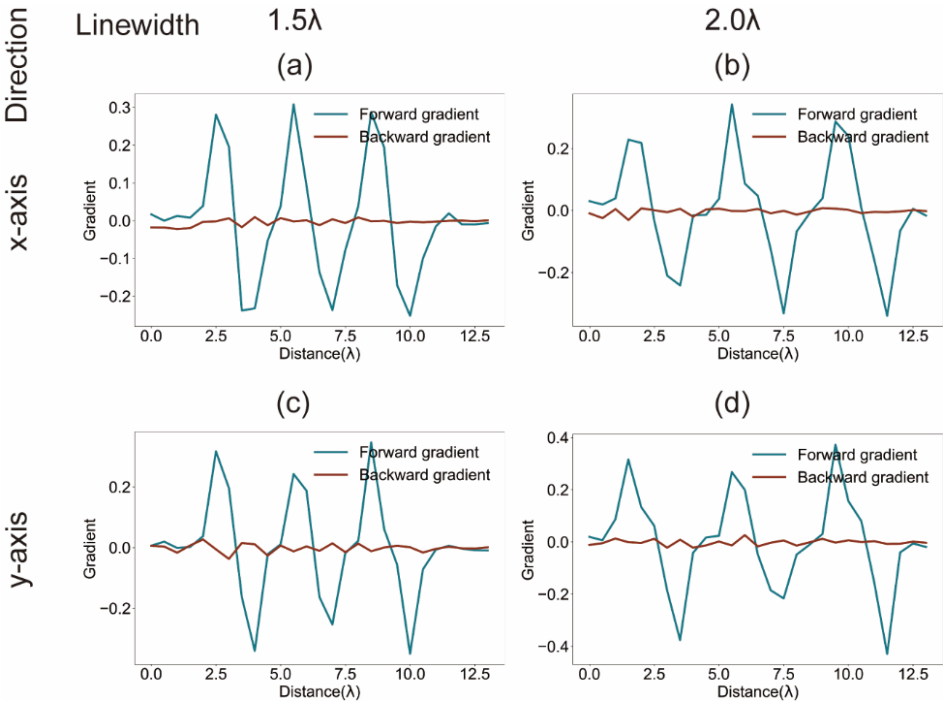

Figure S8. **Gradient analysis using resolution test targets**. (a)-(d) The forward and backward image gradients were calculated to estimate the forward and backward point-spread functions of the unidirectional imager for different resolution test targets with linewidths of 1.5λ and 2.0λ (see Figure 8 of the main text). Each line in (a)-(d) was averaged over the gradients of 5 cross sections evenly spaced within the corresponding resolution test target; each positive and negative peak profile in (a-b) and (c-d) individually represent the effective point spread function along the x- and y-directions, respectively.

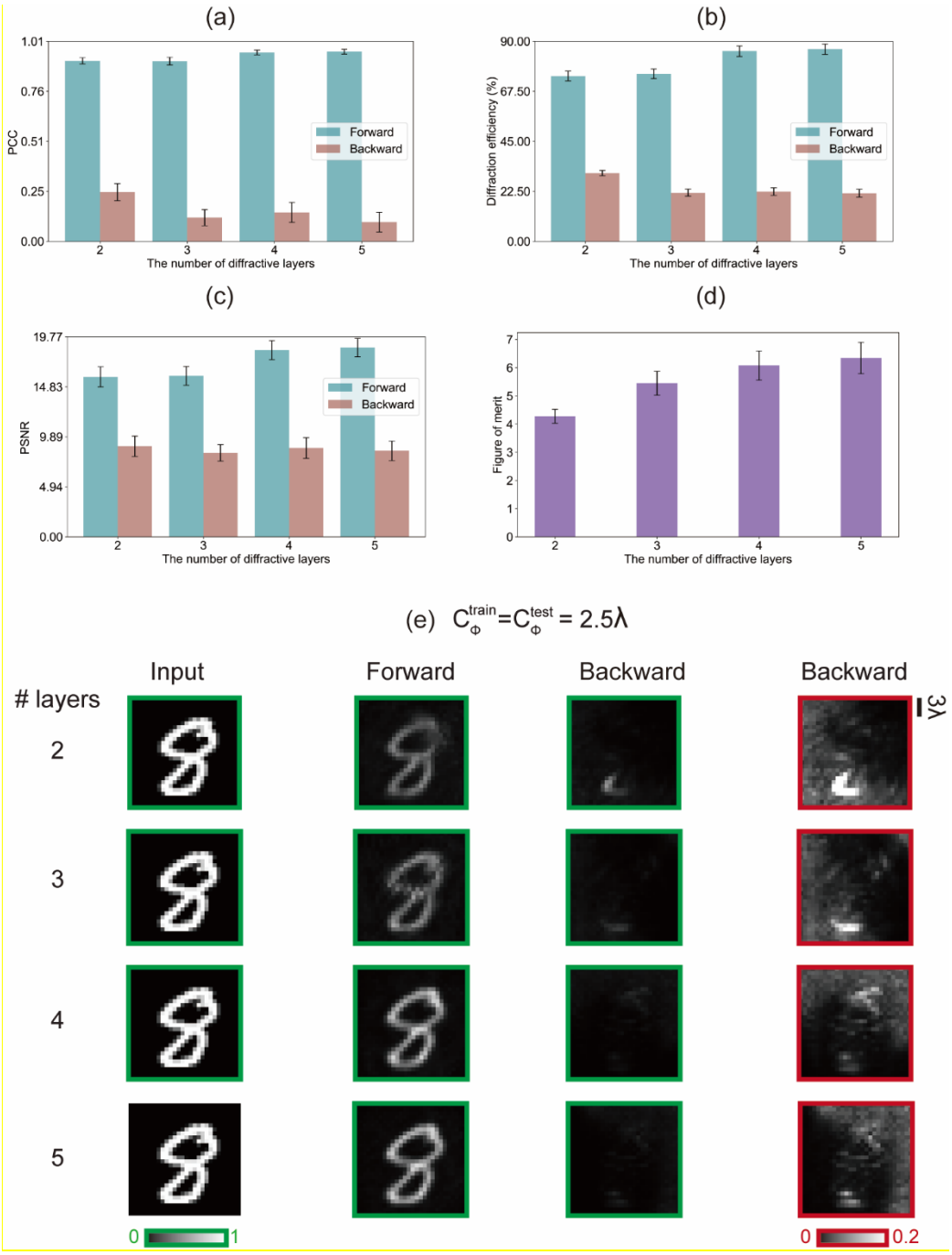

Figure S9. Impact of the number of diffractive layers on the performance of partially coherent unidirectional imagers. (a)-(d) Performance analysis of partially coherent unidirectional diffractive imagers with $C_\Phi^{train} = C_\Phi^{test} = 2.5\lambda$, $N_\Phi^{test} = 2048$, and different numbers of diffractive layers ranging from 2 to 5. The performance in each case was evaluated using 10,000 MNIST test images with PCC, diffraction efficiency, PSNR, and FOM metrics reported. (e) Examples of the blinding testing results with different numbers of diffractive layers. The first three rows display the input amplitude objects, forward

output images, and backward output images, respectively, all using the same intensity range. For comparison, the last row shows the backward output images with an increased contrast.

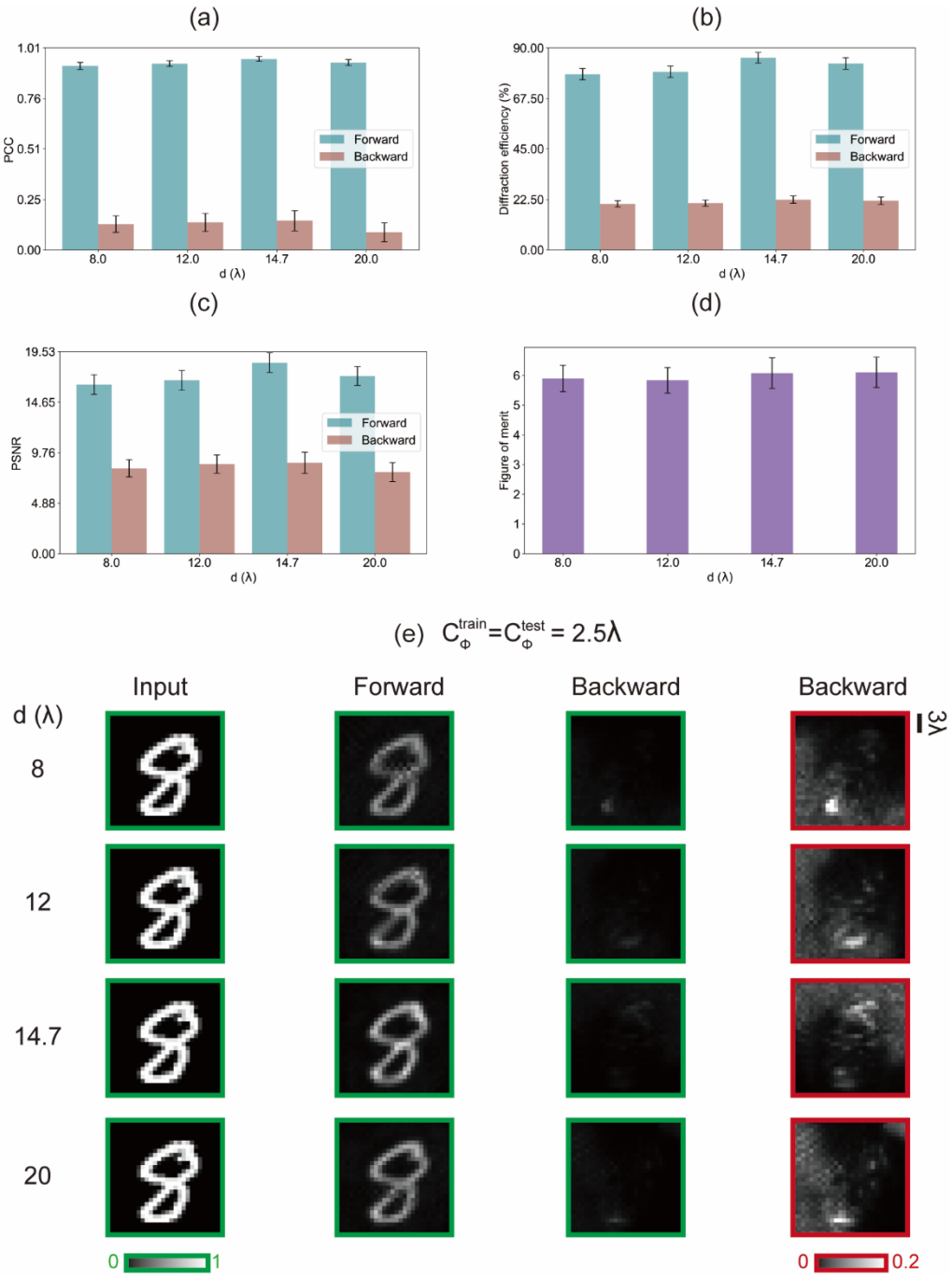

Figure S10. Impact of the layer-to-layer distance on the performance of partially coherent unidirectional imagers. (a)-(d) Performance analysis of partially coherent unidirectional diffractive imagers with $C_\phi^{train} = C_\phi^{test} = 2.5\lambda$, $N_\phi^{test} = 2048$, and different layer-to-layer distances ranging from $8\,\lambda$ to $20\,\lambda$. The

performance in each case was evaluated using 10,000 MNIST test images with PCC, diffraction efficiency, PSNR, and FOM metrics reported. (e) Examples of the blinding testing results with different layer-to-layer distances. The first three columns display the input amplitude objects, forward output images, and backward output images, respectively, all using the same intensity range. For comparison, the last column shows the backward output images with an increased contrast.